Development of novel processable electron accepting conjugated polymers containing fluoranthene units in the main chain

Arne Palmaerts [a], Laurence Lutsen [b], Thomas J. Cleij [a,*], Dirk Vanderzande [a,b], Almantas Pivrikas [c], Helmut Neugebauer [c], Niyazi Serdar Sariciftci [c]

[a] Hasselt University, Institute for Materials Research (IMO), Agoralaan, Building D, B-3590 Diepenbeek, Belgium
[b] IMEC, Division IMOMEC, Wetenschapspark 1, B-3590 Diepenbeek, Belgium
[c] Johannes Kepler University, Department of Physical Chemistry and Linz Institute for Organic Solar Cells (LIOS), Altenberger Strasse 69, A-4040 Linz, Austria

ARTICLE INFO

ABSTRACT

Considerable interest exists in the development of novel n-type conjugated polymers, since many currently available polymer systems have insufficient electron mobility and/or electron affinity. In this work, a universal synthesis route is presented towards a new class of n-type conjugated polymers, i.e. poly(p-fluoranthene vinylene) (PFV) and its derivatives. This route is illustrated with three examples, i.e. unsubstituted PFV and functionalized hexyl-PFV and dodecyl-PFV. All polymers have been synthesized via the dithiocarbamate precursor route. Solubility was introduced by incorporation of alkyl side chains, which leads to a significantly enhanced purity and processability as compared to unsubstituted PFV. Under the applied electrochemical conditions PFV-type polymers demonstrate typical n-type behavior. Additional CELIV mobility measurements on dodecyl-PFV reveal an excellent electron mobility, $\mu_e = 1.4 \times 10^{-4}$ cm^2/Vs. Hence, poly(p-fluoranthene vinylene) and its derivatives are promising n-type materials for organic optoelectronic applications.

© 2009 Elsevier Ltd. All rights reserved.

1. Introduction

Conjugated polymers are important materials for the development of a variety of advanced optical and electronic applications. Whereas some of these applications are already commercially available, for many other applications the currently available conjugated polymers do not yet have suitable properties for optimal device performance. Hence, a quest for new conjugated polymers with enhanced properties continues. Special interest exists for n-type conjugated polymers, since the majority of known conjugated polymers exhibit p-type characteristics. Notwithstanding, n-type materials are of significant importance for, amongst others, the development of n-type polymer field-effect transistors (FETs) and organic photovoltaics.

For FET applications a variety of low molecular weight organic molecules have been identified, which have sufficient charge carrier mobility [1–4]. However, polymeric alternatives are desirable, since they, amongst others, hold significant promise for straightforward and low-cost processing and manufacturing. For example, polymeric materials can be solution processed to devices with a large area. However, only a limited number of n-type conjugated polymers is available [5–16] and two important challenges concerning electron injection and transport remain, i.e. the achievement of a sufficiently high electron affinity and electron mobility. The same two challenges are also valid for organic photovoltaics. Organic photovoltaics offer significant technological potential as an alternative renewable source for electrical energy. Solar cells based on conjugated polymeric materials have several advantages, such as potential flexibility, low manufacturing costs and straightforward processing [17–20]. In most examples of current organic solar cells, a p-type conjugated polymer is combined with a soluble derivative of C$_{60}$, PCBM, as the electron acceptor. However, a polymeric alternative for PCBM can be of interest for a variety of reasons. First of all, it may facilitate the formation of an optimal and more stable morphology [17,21], combined with straightforward large area processing. Furthermore, in polymer–fullerene solar cells a comparatively poor overlap exists between the solar spectrum and the optical absorption of the used materials. It is anticipated that the use of polymer–polymer solar cells will lead to an increase of the photon harvesting, which in turn will lead to an improved performance [22–24].

A wide variety of n-type conjugated polymers have been reported in the literature. In general, these n-type polymers can be divided into two different classes. In the first class the n-type behavior is achieved by the introduction of electron accepting substituents attached to the polymer backbone. One of the most common examples is the introduction of cyano groups, which can increase the electron affinity of a wide variety of conjugated polymers significantly [5–10]. In the

R = H   PFV
R = C$_6$H$_{13}$ hexyl-PFV
R = C$_{12}$H$_{25}$ dodecyl-PFV
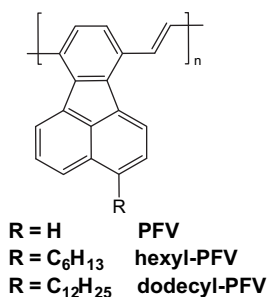
Fig. 1. Chemical structure of the conjugated polymer PFV and its substituted derivatives hexyl-PFV and dodecyl-PFV.

second class, the enhanced electron affinity is related to nitrogen and/or sulfur containing aromatic building blocks [11–16]. Notwithstanding this wide variety of n-type conjugated polymers, for example, the efficiencies of all-polymer solar cells remain rather low as compared to their fullerene containing counterparts. This can be partially explained by the unbalanced charge transport, which is amongst others the result of a low dissociation efficiency and a low mobility in the n-type phase due to the presence of electron traps [25]. Even without focusing on organic solar cells, it appears evident that several of the above mentioned polymer systems suffer from the previously cited challenges, i.e. insufficient electron mobility and/or electron affinity. This prompted our quest for an entirely different class of n-type conjugated polymers.

Recently, we reported on the synthesis of a PPV-type polymer with a new backbone architecture, i.e. poly(p-fluoranthene vinylene) PFV. This polymer was inspired by the progress, which has been made in the synthesis of substructures of C$_{60}$ by researchers in the field of non-alternant hydrocarbons [26]. In the backbone of this conjugated polymer a small substructure of C$_{60}$, i.e. fluoranthene, is incorporated [27]. The resulting PFV exhibits the desired n-type behavior, although many of its other properties remain similar to those of its "parent" polymer PPV. The n-type character is associated with the non-alternant character of the repeating units. Unfortunately, the solubility of PFV as well as its precursors is rather low, complicating synthesis and purification procedures. As a result, incorporation into actual devices has proven troublesome. Hence, the development of more soluble derivatives of PFV is of paramount importance.

In this work, a new and universal synthesis route is presented towards PFV and its derivatives. This route is illustrated for three conjugated polymers, i.e. unsubstituted PFV and functionalized hexyl-poly(p-fluoranthene vinylene) and dodecyl poly(p-fluoranthene vinylene) (Fig. 1). The latter two polymers contain alkyl side chains. It is demonstrated that as a result of these side chains the solubility is considerably improved, leading to enhanced purity and physical properties. All polymers were synthesized via the dithiocarbamate precursor route [28–32]. The optical and electronic properties of these polymers were compared using UV–Vis absorption spectroscopy and cyclic voltammetry. As a result of the enhanced purity, especially dodecyl-PFV is a promising material for optical and electronic applications. Therefore, a first evaluation of charge carrier mobility by CELIV-measurements of dodecyl-PFV will be presented, which demonstrates the suitability of this novel material as an n-type material in optoelectronic applications.

2. Experimental section

2.1. General

NMR spectra were recorded with a Varian Inova Spectrometer (^{1}H NMR 300 MHz, ^{13}C NMR 75 MHz). Analytical Size Exclusion Chromatography (SEC) was performed using a Spectra series P100 (Spectra Physics) pump equipped with two mixed-B columns (10 μm, 2 × 30 cm, Polymer Labs) and a Refractive Index detector (Shodex) at 40 °C or 70 °C. THF or a DMF solution of oxalic acid (1.1 × 10^{-3} M) was used as the eluent at a flow rate of 1.0 mL/min. Molecular weight distributions are given relative to polystyrene standards. Gas chromatography/mass spectrometry (GC/MS) analyses were carried out on TSQ-70 and Voyager mass spectrometers (Thermoquest); the capillary column was a Chrompack Cpsil5CB or Cpsil8CB. DIP-MS measurements were performed at a heating rate of 10 °C/min up to 600 °C. Liberated products were ionized by electron impact. FT-IR spectra were collected with a Perkin Elmer Spectrum One spectrometer (nominal resolution 4 cm^{-1}, summation of 16 scans). UV–Vis measurements were performed on a Cary 500 UV–Vis–NIR spectrophotometer (scan rate 600 nm/min, continuous run from 200 to 600 nm). The conversions of the precursor polymers into the corresponding conjugated structures were followed in situ with FT-IR and UV–Vis spectroscopy. The in-situ FT-IR elimination reactions in the solid state were performed in a Harrick variable temperature cell (Safir), positioned in the beam of the FT-IR spectrometer. The temperature of the sample was controlled by a Watlow (serial number 999, dual channel) temperature controller. The precursor polymer was drop-casted from a CHCl$_3$ solution on a KBr pellet (diameter 25 mm, thickness 1 mm). Afterwards, the KBr-pellet was brought into the cell, which was continuously flushed with nitrogen (open system). The spincoated KBr pellet was in direct contact with the heating element. The in-situ UV–Vis measurements in the solid state were performed in a similar Harrick variable temperature cell as was used for the FT-IR measurements, which was for the UV–Vis measurements positioned in the beam of the UV–Vis–NIR spectrometer. The precursor polymer was drop-casted from a CHCl$_3$ solution on a quartz glass (diameter 25 mm, thickness 3 mm). The experiments were performed in the same manner as the in-situ FT-IR measurements. All measurements were performed under a continuous flow of nitrogen. Electrochemical properties were measured with an Eco Chemie Autolab PGSTAT 20 Potentiostat/Galvanostat using a conventional three-electrode cell (electrolyte: 0.1 M TBAPF$_6$ in anhydrous CH$_3$CN) with an Ag/AgNO$_3$ reference electrode (0.01 M AgNO$_3$, 0.1 M TBAPF$_6$ and CH$_3$CN), a platinum counter electrode and a platinum or Indium–Tin Oxide (ITO) coated glass substrate as working electrode. Cyclic voltammograms were recorded at 50 mV/s under N$_2$ atmosphere. All electrochemical potentials have been referenced to a known standard, ferrocene/ferrocinium, which is estimated to have an oxidation potential of −4.98 V vs. vacuum. Unless stated otherwise, all reagents and chemicals were obtained from commercial sources and used without further purification. Tetrahydrofuran (THF) was purified by distillation from sodium/benzophenone.

2.2. Synthesis (Scheme 1)

Compounds **3a**, **4a**, **5a**, **6a** as well as PFV were prepared as described previously by us [27].

2.2.1. 1-Hexylnaphthalene (1b)

100 mL of a 2 M solution of hexylmagnesiumbromide in diethyl ether was added drop wise to a stirred mixture of 1-bromonaphthalene (29.6 g, 0.143 mol) and Ni(dppp)Cl$_2$ (0.77 g, 0.00143 mol) in diethyl ether (150 mL) while maintaining the temperature below 30 °C. After stirring overnight at room temperature, 2 M aqueous HCl (572 mL) was slowly added after which the resulting layers were separated. The water layer was extracted with diethyl ether (3 × 300 mL). The combined organic layers were washed with a saturated NaHCO$_3$ solution (3 × 200 mL) and dried over anhydrous MgSO$_4$. The solvent was evaporated under reduced pressure
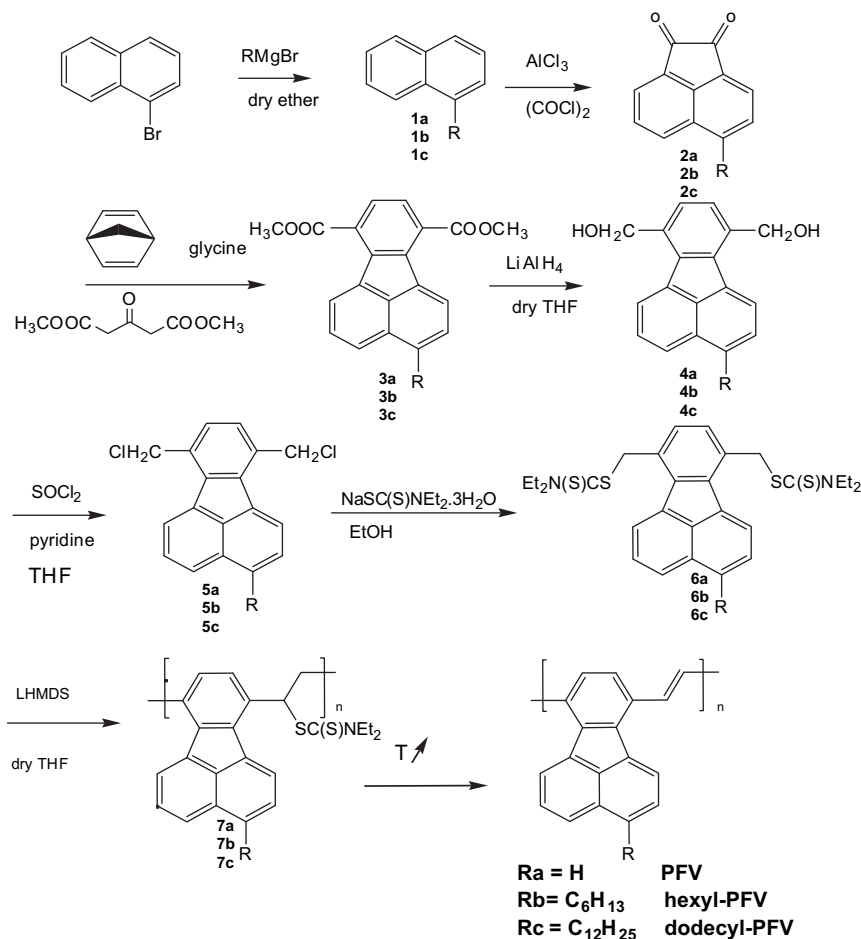
Scheme 1. Synthesis of PFV, hexyl-PFV and dodecyl-PFV.

and the mixture was further purified by kugelrohr distillation to give 29.5 g of a white solid product (97% yield). ^{1}H NMR (CDCl$_3$): $\delta = 8.12$ (d, 1H), 7.91 (dd, 1H), 7.77 (d, 1H), 7.55 (m, 2H), 7.46 (t, 1H), 7.38(d, 1H), 3.13 (t, 2H), 1.79 (m, 2H), 1.54–1.34 (br, m, 6H), 0.99 (t, 3H); ^{13}C NMR (CDCl$_3$): $\delta = 138.9$, 133.8, 131.8, 128.6, 126.3, 125.7, 125.5, 125.4, 125.2, 123.8, 33.0, 31.7, 30.8, 29.5, 22.6, 14.0.

2.2.2. 1-Dodecylnaphthalene (**1c**)

Starting from 600 mL of a 1 M solution of dodecylmagnsesiumbromide in diethyl ether, 1-bromonaphthalene (1.05 g, 0.507 mol) and Ni(dppp)Cl$_2$ (2.74 g, 0.00507 mol) dissolved in 600 mL of diethyl ether and 2 M aqueous HCl (2 L) using a similar procedure as described for **1b**, compound **1c** was obtained as a white solid. (144 g, 96% yield). ^{1}H NMR (CDCl$_3$): $\delta = 8.08$ (d, 1H), 7.88 (dd, 1H), 7.73 (d, 1H), 7.51 (m, 2H), 7.42 (t, 1H), 7.35 (d, 1H), 3.10 (t, 2H), 1.79 (m, 2H), 1.62–1.21 (br m, 18 H), 0.94 (t, 3H); ^{13}C NMR (CDCl$_3$): $\delta = 138.9$, 133.8, 131.8, 128.6, 126.3, 125.7, 125.5, 125.4, 125.2, 123.8, 33.1, 31.9, 30.9, 29.8, 29.7, 29.7, 29.6, 29.6, 29.5, 29.3, 22.7, 14.1.

2.2.3. 5-Hexylacenaphthylene-1,2-dione (**2b**)

Oxalyl chloride (8.98 g, 0.0708 mol) was added to a stirred suspension of AlCl$_3$ (28 g, 0.212 mol) in 1,2-dichloroethane (300 mL) at 0 °C. After the drop wise addition of **1b** (15 g, 0.0708 mol) in 1,2-dichloroethane (50 mL) the stirring was continued for 6 h at the same temperature. The reaction mixture was quenched with water (200 mL) and the resulting layers were separated. Subsequently the organic layer was washed with an aqueous 2 M solution of sodium

carbonate (1 × 200 mL) and water (1 × 300 mL) after which it was dried over anhydrous MgSO$_4$. After removal of the solvent at reduced pressure, the crude product was further purified by column chromatography (silica, CH$_2$Cl$_2$) to give 4.15 g **2b** as yellow crystals (22% yield). ^{1}H NMR (CDCl$_3$): $\delta = 8.33$ (d, 1H), 8.01 (t, 2H), 7.80 (t, 1H), 7.61 (d, 1H), 3.16 (t, 2H) 1.77 (m, 2H), 1.46–1.23 (br, m, 6H), 0.87 (t, 3H); ^{13}C NMR (CDCl$_3$): $\delta = 188.8$, 187.6, 147.4, 146.1, 129.7, 129.5, 128.7, 127.8, 127.8, 126.8, 122.1, 121.4, 32.9, 31.5, 30.4, 29.2, 22.4, 13.9.

2.2.4. 5-Dodecyl-acenaphthylene-1,2-dione (**2c**)

Starting from oxalyl chloride (6.43 g, 0.0507 mol), AlCl$_3$ (20.27 g, 0.152 mol) and **1c** (15 g, 0.0507 mol), using a similar procedure as described for **2b**, compound **2c** was obtained as yellow crystals (4.01 g, 22% yield). ^{1}H NMR (CDCl$_3$) $\delta = 8.35$ (d, 1H), 8.06 (d, 1H), 8.03 (d, 1H), 7.82 (dd, 1H), 7.64 (d, 1H), 3.18 (t, 2H), 1.78 (p, 2H), 1.49–1.28 (br m, 18H), 0.85 (t, 3H); ^{13}C NMR (CDCl$_3$): $\delta = 188.6$, 187.4, 147.4, 146.0, 129.6, 129.5, 128.6, 127.7, 127.7, 126.7, 122.0, 121.3, 32.8, 31.7, 30.4, 29.5, 29.4, 29.4, 29.4, 29.4, 29.3, 29.1, 22.5, 13.9.

2.2.5. 3-Hexylfluoranthene-7,10-dicarboxylic acid dimethyl ester (**3b**)

A mixture of **2b** (3.0 g, 11.28 mmol), dimethyl 1,3-acetone dicarboxylate (4.7 g, 26.99 mmol) and glycine (1.86 g, 24.78 mmol) in 2,5-norbornadiene (70 mL) was stirred at reflux temperature for 3.5 days. The reaction flask was equipped with a Dean–Stark trap to remove the water generated from the reaction. Excess solvent was removed at the end of the reaction by simple distillation to give a red-brown solid. The resulting solid was dissolved in CHCl$_2$

(200 mL) and then washed with H_2O (200 mL). After evaporation the product was further purified by column chromatography (silica, CH_2Cl_2) to give 3.72 g of **3b** as yellow crystals (82% yield). ^{1}H NMR ($CDCl_3$): $\delta = 8.59$ (d, 1H), 8.52 (d, 1H), 8.10 (d, 1H), 7.80 (dd, 2H), 7.67 (t, 1H), 7.45 (d, 1H), 4.06 (s, 6H), 3.15 (t, 2H), 1.77 (m, 2H), 1.42–1.19 (br, m, 6H), 0.87 (t, 3H); ^{13}C NMR ($CDCl_3$): $\delta = 168.0$, 167.9, 142.2, 139.5, 139.3, 133.8, 133.4, 131.6, 129.5, 129.0, 128.8, 128.1, 127.5, 127.4, 127.2, 126.4, 125.8, 125.2, 52.5, 52.4, 32.3, 31.9, 31.7, 29.3, 22.6, 14.1.

2.2.6. 3-Dodecylfluoranthene-7,10-dicarboxylic acid dimethyl ester (3c)

Starting from a mixture of **2c** (3.73 g, 10.53 mmol), dimethyl 1,3-acetone dicarboxylate (4.4 g, 25.27 mmol) and glycine (1.73 g, 23.05 mmol) in 2,5-norbornadiene (70 mL), using a similar procedure as described for **3b**, compound **3c** was obtained as yellow crystals (4.15 g, 81% yield). ^{1}H NMR ($CDCl_3$): $\delta = 8.59$ (d, 1H), 8.53 (d, 1H), 8.09 (d, 1H), 7.79 (dd, 2H), 7.66 (t, 1H), 7.45 (d, 1H), 4.06 (s, 6H), 3.14 (t, 2H), 1.77 (m, 2H), 1.49–1.16 (br, m, 6H), 0.87 (t, 3H); ^{13}C NMR ($CDCl_3$): $\delta = 167.9$, 167.8, 142.1, 139.4, 139.3, 133.7, 133.3, 131.4, 129.3, 128.8, 128.7, 128.0, 127.3, 127.3, 127.1, 126.3, 125.7, 125.2, 52.4, 52.3, 33.3, 31.3, 30.2, 29.4, 29.4, 29.3, 29.3, 29.3, 29.2, 29.0, 22.3, 13.7.

2.2.7. 3-Hexyl-7,10-bis(hydroxymethyl) fluoranthene (4b)

A solution of diester **3b** (1 g, 2.49 mmol) in dry THF (50 mL) was added drop wise with stirring to a dispersion of lithium aluminium hydride (0.24 g, 6.25 mmol) in THF (50 mL) at 0 °C. The reaction mixture was allowed to warm to room temperature and stirred for 6 h. Subsequently, water (10 mL), 10% aqueous sodium hydroxide (10 mL) and water (10 mL) were added. After acidification of the water layer to pH = 6 with 1 N HCL the layers were separated and the water layer was extracted with 1:1 ether/THF (3×200 mL). The combined organic layers were washed with water (300 mL), after which they were dried over anhydrous $MgSO_4$. Removal of the solvents under reduced pressure gave a yellow solid, which was further purified by crystallization from methanol to give 0.33 g of **4b** as yellow crystals (38% yield). ^{1}H NMR (DMSO): $\delta = 8.07$ (d, 1H), 8.05 (d, 1H), 7.94 (d, 1H), 7.71 (dd, 1H), 7.50 (d, 1H), 7.47 (s, 2H), 5.43 (m, 2H), 5.00 (t, 4H), 3.11 (t, 2H), 1.70 (m, 2H), 1.43–1.18 (br, m, 6H), 0.84 (t, 3H); ^{13}C NMR (DMSO): $\delta = 139.8$, 137.2, 136.9, 136.4, 135.3, 135.2, 134.1, 131.9, 128.5, 127.8, 127.6, 126.0, 125.7, 124.3, 124.0, 123.5, 61.4, 61.4 31.8, 31.4, 31.2, 28.7, 22.1, 14.0.

2.2.8. 3-Dodecyl-7,10-bis(hydroxymethyl) fluoranthene (4c)

Starting from **3c** (2 g, 4.15 mmol) and $LiAlH_4$ (0.38 g, 9.96 mmol), using a similar procedure as described for **4b**, compound **4c** was obtained as yellow crystals (0.92 g, 52% yield). ^{1}H NMR (DMSO): $\delta = 8.07$ (d, 1H), 8.05 (d, 1H), 7.95 (d, 1H), 7.72 (dd, 1H), 7.50 (d, 1H), 7.47 (s, 2H), 5.42 (m, 2H), 5.00 (t, 4H), 3.13 (t, 2H), 1.72 (m, 2H), 1.49–1.13 (br, m, 18H), 0.84 (t, 3H). ^{13}C NMR (DMSO): $\delta = 139.8$, 137.2, 136.9, 136.4, 135.3, 135.2, 134.1, 131.9, 128.5, 127.8, 127.6, 126.0, 125.7, 124.3, 124.0, 123.5, 61.4, 61.4, 31.8, 31.4, 31.3, 30.4, 29.0, 28.8, 28.7, 28.6, 28.5, 28.4, 22.1, 14.0.

2.2.9. 3-Hexyl-7,10-bis(chloromethyl) fluoranthene (5b)

Thionylchloride (0.38 g, 3.18 mmol) was added drop wise to a solution of the diol **4b** (0.5 g, 1.45 mmol) and pyridine (0.46 g, 5.78 mmol) in THF (80 mL) at 0 °C. The mixture was stirred at reflux temperature for 24 h. After dilution with water (150 mL) and extraction with $CHCl_3$ (3×200 mL), the combined organic layers were dried over $MgSO_4$ and the solvent was evaporated. The resulting product was further purified by crystallization from CH_2Cl_2 to give 0.35 g of **5b** as light yellow crystals (63% yield). ^{1}H NMR ($CDCl_3$): $\delta = 8.11$ (d, 1H), 8.03 (t, 2H), 7.68 (t, 1H), 7.46 (d, 1H), 7.28 (s, 2H), 5.02 (s, 2H), 5.01 (s, 2H), 3.13 (t, 2H), 1.78 (m, 2H), 1.44–1.23 (br, m, 6H), 0.89 (t, 3H); ^{13}C NMR ($CDCl_3$): $\delta = 141.3$, 138.1, 138.0, 135.3, 133.0, 132.7, 128.9, 128.6, 127.6, 127.5, 124.4, 124.3, 123.9, 44.5, 44.5, 32.2, 31.9, 31.6, 29.2, 22.5, 14.0.

2.2.10. 3-Dodecyl-7,10-bis(chloromethyl) fluoranthene (5c)

Starting from **4c** (2.1 g, 4.88 mmol), thionylchloride (1.54 g, 19.5 mmol) and pyridine (1.28 g, 10.7 mmol), using a similar procedure as described for **5b**, compound **5c** was obtained as light yellow crystals (1.52 g, 67% yield). ^{1}H NMR ($CDCl_3$): $\delta = 8.16$ (d, 1H), 8.08 (d, 1H), 8.05 (d, 1H), 7.70 (dd, 1H), 7.48 (d, 1H), 7.32 (s, 1H), 7.32 (s, 1H), 5.07 (s, 2H), 5.06 (s, 2H), 3.15 (t, 2H), 1.78 (m, 2H), 1.52–1.17 (br m, 18H), 0.86 (t, 3H); ^{13}C NMR: ($CDCl_3$): $\delta = 141.3$, 138.2, 138.0, 135.4, 133.1, 132.7, 129.0, 128.6, 127.6, 127.5, 124.4, 124.3, 123.9, 44.5, 44.5, 32.2, 31.9, 31.7, 29.5, 29.5, 29.4, 29.4, 29.3, 29.3, 29.2, 22.5, 14.0.

2.2.11. 3-Hexyl-7,10-bis((N,N-diethyl dithiocarbamate)-methyl)fluoranthene (6b)

A mixture of dichloride **5b** (0.3 g, 0.78 mmol), sodium diethyldithiocarbamate trihydrate (0.53 g, 2.35 mmol) in ethanol (80 mL) was stirred at room temperature for 24 h. Subsequently, water (50 mL) was added after which the desired monomer was extracted with chloroform (3×150 mL). The combined $CHCl_3$ layers were dried over $MgSO_4$ and after evaporation of the solvent the crude monomer was obtained. Further crystallization from methanol yielded 0.34 g of pure **6b** as light yellow crystals (72% yield). ^{1}H NMR ($CDCl_3$): $\delta = 8.06$ (d, 1H), 7.98 (dd, 2H), 7.64 (dd, 1H), 7.43 (d, 1H), 7.31 (s, 2H), 4.94 (s, 2H), 4.93 (s, 2H), 4.07 (dd, 4H), 3.67 (dd, 4H), 3.12 (t, 2H), 1.76 (m, 2H), 1.44–1.23 (br, m, 6H), 1.20 (t, 6H) 0.87 (t, 3H); ^{13}C NMR ($CDCl_3$) $\delta = 195.1$, 195.1, 140.6, 138.4, 138.2, 135.9, 133.6, 132.8, 130.2, 130.0, 129.9, 129.6, 128.9, 127.6, 127.5, 124.1, 123.8, 123.7, 49.2, 49.2, 46.6, 46.6, 41.2, 41.2, 32.2, 31.9, 31.6, 29.2, 22.5, 13.4, 12.3, 12.3, 11.5, 11.5; GC-MS (EI, m/e): 608 (M^+), 460 (M^+-SC(S)NEt_2), 312 (M^+-$2 \times$ SC(S)NEt_2), 242 (M^+-SC(S)NEt_2–C_5H_{13}), 148 (SC(S)NEt_2), 116 (C(S)NEt_2), 72 (NEt_2); FT-IR (NaCl, cm^{-1}): 2959, 2924, 2853, 1486, 1457, 1415, 1318, 1354, 1305, 1269, 1204, 1141, 1068, 1009, 982, 918, 830, 759.

2.2.12. 3-Dodecyl-7,10-bis((N,N-diethyl dithiocarbamate)-methyl)fluoranthene (6c)

Starting from **5c** (1.5 g, 3.21 mmol) and sodium diethyldithiocarbamate trihydrate (3.6 g, 16.0 mmol), using a similar procedure as described for **6b**, compound **6c** was obtained as light yellow crystals (1.48 g, 76% yield). ^{1}H NMR ($CDCl_3$): $\delta = 8.04$ (d, 1H), 7.97 (dd, 2H), 7.64 (dd, 1H), 7.42 (d, 1H), 7.30 (s, 2H), 4.93 (s, 4H), 4.07 (d, 4H), 3.65 (d, 4H), 3.11 (t, 2H), 1.76 (m, 2H), 1.51–1.16 (br m, 30H), 0.87 (t, 3H); ^{13}C NMR ($CDCl_3$): $\delta = 195.1$, 195.1, 140.6, 138.4, 138.2, 135.9, 133.6, 132.8, 130.2, 130.0, 129.9, 129.6, 128.9, 127.6, 127.5, 124.1, 123.8, 123.7, 49.2, 49.2, 46.6, 46.6, 41.2, 41.2, 32.2, 31.9, 31.8, 29.5, 29.5, 29.5, 29.4, 29.4, 29.3, 29.2, 22.6, 14.0, 12.3, 12.3, 11.5, 11.5; GC-MS (EI, m/e): 692 (M^+), 544 (M^+-SC(S)NEt_2), 396 (M^+-$2 \times$ SC(S)NEt_2), 242 (M^+-SC(S)NEt_2–$C_{11}H_{25}$), 148 (SC(S)NEt_2), 116 (C(S)NEt_2), 72 (NEt_2); FT-IR (NaCl, cm^{-1}): 2960, 2925, 2852, 1593, 1485, 1455, 1430, 1415, 1378, 1354, 1300, 1268, 1205, 1142, 1068, 1008, 984, 917, 829, 762.

2.2.13. Precursor polymer for hexyl-poly(p-fluoranthene vinylene) (7b)

A solution of monomer **6b** (0.3 g, 0.49 mmol) in dry THF (2.47 mL) was degassed for 1 h by passing through a continuous N_2 flow. Subsequently, 0.78 mL of a 1 M LHMDS solution in THF was added in one go to the stirred monomer solution. The mixture was stirred for an additional 3 h under N_2 atmosphere after which the polymer was precipitated in ice water and subsequently extracted with chloroform (3×200 mL). The solvent of the combined organic layers was evaporated under reduced pressure. After dissolving the precursor polymer in a small amount of $CHCl_3$, **7b** was isolated by

precipitation in methanol. After further purifications by soxhlet extractions with MeOH, hexane and acetone, respectively, to remove low molecular weight contaminants and/or oligomers, 143 mg of the pure precursor polymer **7b** was isolated as a light yellow solid (62% yield). ^{1}H NMR (CDCl$_3$): δ = 8.8–6.0 (b, 7H), 4.4–2.4 (b, 9H), 2.0–0.2 (b, 17H); SEC (THF) M_w = 2.7 × 10^5 g/mol (PD = M_w/M_n = 2.8); FT-IR (NaCl, cm^{-1}): 2954, 2928, 2856, 1486, 1456, 1430, 1416, 1354, 1266, 1206, 1142, 1074, 1010, 916, 830.

2.2.14. Precursor polymer for dodecyl-poly(p-fluoranthene vinylene) (7c)

Starting from monomer **6c** (0.2 g, 0.29 mmol) and 0.46 mL of a 1 M LHMDS solution in THF, using a similar procedure as described for **7b**, precursor polymer **7c** was obtained as a light yellow solid (92 mg, 58% yield). ^{1}H NMR (CDCl$_3$): δ = 9.0–6.0 (b, 7H), 4.4–2.4 (b, 9H), 2.2–0.2 (b, 29H); SEC (THF) M_w = 2.3 × 10^5 g/mol (PD = M_w/M_n = 2.1); FT-IR (NaCl, cm^{-1}): 2924, 2850, 1486, 1458, 1431, 1417, 1354, 1266, 1206, 1142, 1074, 1010, 916, 830.

2.2.15. Thermal conversion of 7a, 7b and 7c into the corresponding conjugated form (PFV, hexyl-PFV and dodecyl-PFV)

Thin films of precursor polymers **7a**, **7b** and **7c** have been converted into the conjugated polymers PFV, hexyl-PFV and dodecyl-PFV by a thermal treatment under N$_2$ atmosphere. During this treatment the dithiocarbamate group is eliminated from the precursor polymers. For the thermal treatment, the precursor polymers **7a**, **7b** and **7c** were spin-coated from CHCl$_3$ solutions onto a suitable substrate. Subsequently, these coated substrates were placed in a controlled temperature cell and were heated to a suitable conversion temperature (*e.g.* 165 °C). Hexyl-PFV and dodecyl-PFV were obtained as yellow-orange solids. Hexyl-PFV: FT-IR (NaCl, cm^{-1}): 2956, 2928, 2856, 1430, 960, 822, 808, 750. Dodecyl-PFV: FT-IR (NaCl, cm^{-1}): 2924, 2852, 1430, 958, 822, 808, 750.

2.3. Mobility measurements

Sandwich-type samples were prepared for charge carrier mobility measurements of dodecyl-PFV. To this end, the precursor polymer **7c** was dissolved in chloroform (40 mg/mL). The solution was filtered through a 0.45 μm filter before deposition by spin coating on top of prepatterned ITO-covered glass substrates. A film thickness of 400 nm was used to avoid the presence of pinholes. Subsequently, the precursor polymer was converted to the conjugated dodecyl-PFV (*vide supra*) and 100 nm aluminium top contacts were evaporated on top of the polymer (vacuum 10^{-6} mbar). Samples were prepared under inert atmosphere and the films were measured *in vacuo* using an optical cryostat (Oxford Optistat DNV). For the CELIV experiments a variable pulse generator (Agilent 33250A) and oscilloscope (Tektronix TDS 754C) were used to record the current transients. For triggering purposes to ensure the proper delay time between voltage and light pulse, a pulse and the delay function generator (Stanford DG535) were used. A Nd:YAG laser (Coherent Infinity 40–100) was employed to photogenerate the charge carriers using a 5 ns laser pulse at a wavelength of 355 nm and an intensity of less than 1 mJ/pulse per standard laser beam output area. The films were illuminated through the ITO side when forward and reverse voltage was applied to the sample.

3. Results and discussion

3.1. Monomer synthesis (Scheme 1)

Since for production of optoelectronic devices soluble polymers are needed, various strategies have been explored to achieve this. One possibility to overcome the solubility issue is the use of a precursor route for the polymerization [28–32]. With such a route a soluble non-conjugated precursor polymer is obtained, which subsequently can be converted into its conjugated form *in situ*. This approach has been utilized to obtain thin films of the unsubstituted PFV. However, unfortunately even the solubility of the precursor polymer of PFV is insufficient to obtain thin films of sufficient quality for device applications. Therefore as an alternative, long flexible solubilizing side chains have been introduced and the synthesis procedure has been optimized, giving the functionalized hexyl-PFV and dodecyl-PFV. The synthesis of these alkyl-PFV derivatives starts with the virtually quantitative Grignard reaction between magnesium alkyl bromide and bromonaphthalene. Subsequently, these alkyl naphthalenes **1b** and **1c** have been converted into the acenaphthenequinone derivatives **2b** and **2c** using a double Friedel-Crafts acylation. The further steps of the monomer synthesis are similar as described previously by us for the monomer of PFV [27]. It is comprised of a straightforward one-step synthesis of the dimethyl fluoranthene-7,10-dicarboxylic esters **3a**, **3b** and **3c** from the corresponding acenaphtenequinone derivatives, acetone dicarboxylic ester and norbornadiene, followed by the reduction with LiAlH$_4$ of the ester groups giving the diols **4a**, **4b** and **4c** according to a literature procedure [26]. Subsequently, the 7,10-bis(chloromethyl)fluoranthene derivatives **5a**, **5b** and **5c** were obtained by reaction with thionylchloride in THF solution. Whereas the rather limited solubility of **4a** and **5a** required the use of dilute solutions, this is not the case for the alkyl substituted derivatives. Finally, the monomers for the dithiocarbamate precursor route were synthesized by reaction with sodium diethyldithiocarbamate trihydrate, giving the monomers **6a**, **6b** and **6c** as light yellow crystalline solids in excellent yield.

3.2. Polymerization

For the polymerization, the dithiocarbamate precursor route was chosen [28–32], which was previously developed in our laboratory. This route offers not only a straightforward monomer synthesis, but also precursor polymers of higher quality than many other available precursor routes [29]. Hence, a polymerization can be accomplished in a straightforward manner. The use of a precursor route can also have advantages for the ultimate device stability, which is of crucial importance in organic electronics [33]. First of all, a precursor route offers a pathway towards good processing properties, as will be demonstrated for the PFV derivatives (*vide infra*). In addition, the precursor route has the potential to provide better device stability due to the possibility to remove part of the solubilizing groups, *i.e.* the dithiocarbamate groups, from the final conjugated polymer by post polymerization elimination. Such post polymerization processing procedures of conjugated polymer films are highly promising for device applications [34–36].

Polymerization of **6a**, **6b** and **6c** was carried out with lithium bis(trimethylsilyl) amide (LHMDS) as the base in dry THF under inert atmosphere (Scheme 1). After extraction the precursor polymers **7a**, **7b** and **7c** were isolated in excellent yield by precipitation in MeOH. Further purifications by soxhlet extractions in MeOH, hexane and acetone have been utilized to remove low molecular weight contaminants and/or oligomers.

Selected polymerization results are presented in Table 1. The weight-average molecular weights (M_w) of the precursor polymers have been determined by analytical SEC in DMF (**7a**) and THF (**7b** and **7c**) using polystyrene standards. In view of the differences in solubility, molecular weights of both polymers were measured in different solvents. It should be noted that since all molecular weights are referenced to polystyrene standards, the actual value for M_w will likely somewhat differ from the apparent M_w observed with analytical SEC. The polymerization results clearly demonstrate

Table 1
Selected polymerization results for the synthesis of the precursor polymers **7a**, **7b** and **7c**. Molecular weights are given as determined by analytical SEC in DMF (**7a**) and THF (**7b** and **7c**) using polystyrene standards.

Polymer	M_w ($\times 10^{-3}$)	PD	Yield (%)	Optical band gap (eV)
7a	59	1.6	82	2.3
7b	272	2.8	62	2.2
7c	230	2.1	58	2.2

the significantly enhanced molecular weights of **7b** and **7c**, as compared to **7a**. This is a result of the enhanced purity of the monomers used for the polymerization of **7b** and **7c**, which can be explained by their improved solubility associated with alkyl side chains. The employed synthetic methodology can be regarded as a universal scheme towards a wide variety of substituted PFV derivatives. This is a result of the fact that the first two steps in this scheme, which involve the introduction of the actual substituent, are compatible with a variety of side chains. One can envisage many different types and even numbers of side chains being introduced in this manner, with the hexyl-PFV and dodecyl-PFV presented here being only a proof-of-principle.

3.3. Optical properties

Thin films of the conjugated polymers PFV, hexyl-PFV and dodecyl-PFV have been obtained by a thermal treatment under N_2 atmosphere of the corresponding precursor polymers **7a**, **7b** and **7c**. It was observed that for the polymers the conversion to the conjugated structure started at *circa* 100 °C and was completed at *circa* 150 °C under the thermal conditions used. The converted polymers have an orange color as a result of their π-conjugation. The thin film conversion process can readily be followed by means of *in situ* UV–Vis spectroscopy and FT-IR spectroscopy. For example, upon heating a thin film of **7c** the formation of the conjugated structure of dodecyl-PFV is readily observed (Fig. 2). At low temperatures, in the precursor polymer the long wavelength side of the UV–Vis absorption spectrum is dominated by the typical HOMO–LUMO absorption bands of the substituted fluoranthene at 359 and 380 nm (Fig. 3), which are also present in monomers **6a**, **6b** and **6c**. Upon heating, these bands disappear and two new absorption bands develop, which originate from the conjugated structure. The new band at 320 nm is a result of the more extended conjugated system in this type of polymers [37]. The broad band
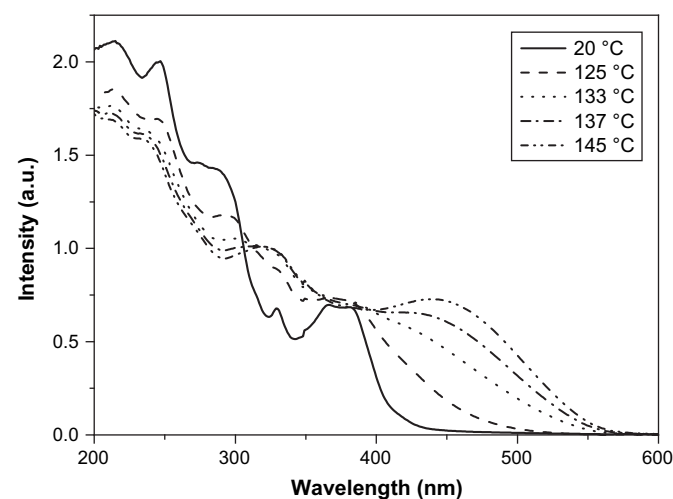
Fig. 2. Temperature-dependent UV–Vis spectra of the conversion of precursor polymer **7c** to dodecyl-PFV at selected temperatures.
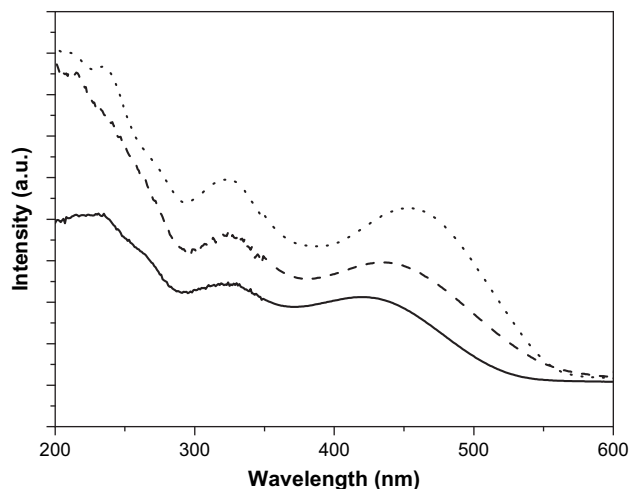

Fig. 3. Comparison of the room temperature UV–Vis absorption spectra of the conjugated polymers PFV (solid line), hexyl-PFV (dashed line) and dodecyl-PFV (dotted line). The intensities of the individual spectra are adjusted to allow for a clear comparison of λ_{max} of the polymers.

around 450 nm can be associated with the π–π* transition ($\lambda_{max} = 420$ nm for PFV, 448 nm for hexyl-PFV and 453 nm for dodecyl-PFV). Although these values are in the same order of magnitude, the absorption maxima of hexyl-PFV and dodecyl-PFV are significantly red shifted as compared to PFV. This is a result of the presence of the alkyl side chains in hexyl-PFV and dodecyl-PFV. The increased solubility of all intermediates during the synthesis, including the monomer and the precursor polymer, as a result of these solubilizing side chains, results in the formation of a better defined precursor polymer. Ultimately, this apparently leads after thermal treatment to a conjugated polymer with a considerably longer effective conjugation length. From the above considerations, it can be concluded that dodecyl-PFV is the PFV derivative with the highest purity. In this context, it should be noted that the actual solubility of the substituted conjugated PFV-derivatives remains not optimal and the polymers remain insufficiently soluble to perform, for example, analytical SEC. Whereas an improved solubility is observed as a result of the introduced side chains, further optimizations of these chains will be required to obtain full solubility in a wide range of solvents.

The optical band gap can be derived from the low energy side tangent to the π–π* transition in the UV–Vis absorption spectrum. In this manner, values for the band gap of *circa* 2.2 eV for PFV, hexyl-PFV and dodecyl-PFV are obtained (Table 1). This indicates that, whereas the position of λ_{max} shifted upon substitution, indicating the presence of less defects in the overall polymer distribution, the onset of absorption, *i.e.* the band gap, is not as much affected, since this is an intrinsic polymer property associated with the longest defect-free polymer segments. The band gap values observed for PFV and its derivatives is only slightly smaller than the reported band gap of PPV (*circa* 2.4 eV) [29,38]. Apparently both the extension of the conjugated system and the functionalization with alkyl side chains, have only a minimal impact on the optical band gap.

To gain a better understanding of the conversion process, the formation of dodecyl-PFV, the PFV derivative with the highest purity, was studied in more detail. From the absorption profile at 453 nm it is evident that conversion of **7c** to its conjugated form starts around 100 °C and is virtually completed at 150 °C (Fig. 4). The apparent minor decrease in absorption at temperatures above 200 °C is a result of a reversible thermochromic effect [39]. Furthermore, the UV–Vis analysis indicates that no degradation of the conjugated structure of dodecyl-PFV is observed in the entire
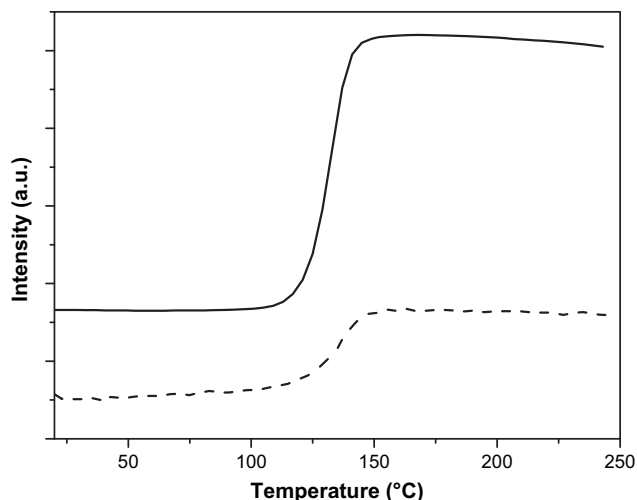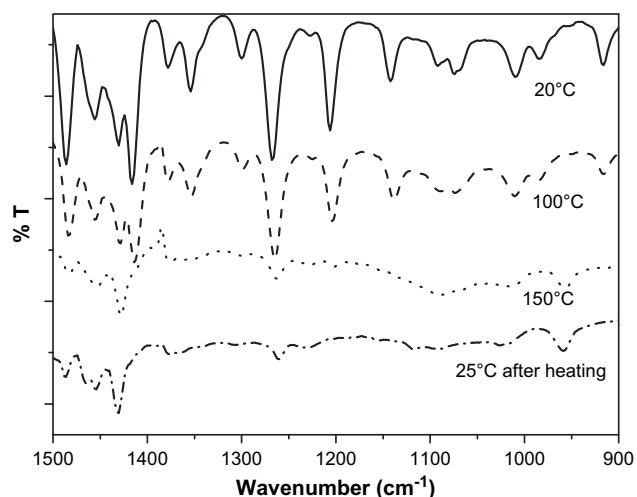
Fig. 4. UV–Vis intensity profile at 453 nm (solid) and FT-IR intensity profile at 958 cm^{-1} (dashed) as a function of temperature during the conversion process of precursor polymer **7c** to dodecyl-PFV.
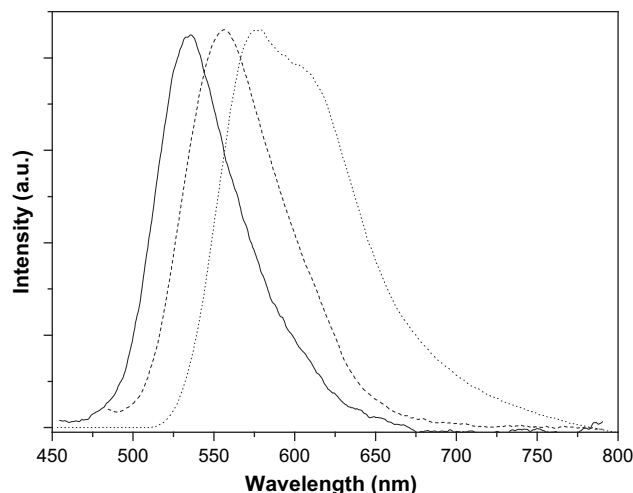

Fig. 6. Comparison of the room temperature fluorescence spectra of thin films of the conjugated polymers PFV (solid line; excitation at 420 nm), hexyl-PFV (dashed line; excitation at 450 nm) and dodecyl-PFV (dotted line; excitation at 453 nm). The intensities of the individual spectra are normalized.

temperature range up to 250 °C. A similar observation can be made for the other PFV-type polymers. Temperature dependent UV–Vis is the analytical method of choice to assess the thermal stability of conjugated polymers [29]. Although the thermal stability of our PFV-derivatives is better than many conjugated polymer systems, this is not unexpected since the base structure, *i.e.* PPV, also has a thermal stability well above 300 °C [29]. Notwithstanding, this confirms that this new class of materials will not exhibit any form of thermal degradation during standard device operations.

The thermal conversion process of **7c** into dodecyl-PFV can also readily be followed using temperature dependant FT-IR spectroscopy (Fig. 5). Upon heating, the vibrations at 1485, 1417, 1266, 1206 cm^{-1}, which are associated with the dithiocarbamate groups, decrease in intensity. At the same time a new vibration develops at 958 cm^{-1}, which arises from the double bonds in the conjugated backbone. The FT-IR measurements confirm that the formation of double bonds starts at 100 °C and is virtually completed around 180 °C with only minimal intensities of the dithiocarbamate groups remaining.

Fluorescence measurements further confirm the successful formation of the conjugated structure. Whereas precursor polymer

7c has a fluorescence emission at $\lambda_{em} = 475$ nm (excitation at $\lambda_{exc} = 380$ nm), which is typical for fluoranthene, this fluorescence is no longer present in the corresponding conjugated polymer. Instead for dodecyl-PFV a distinct emission with a yellow color is found at $\lambda_{em} = 576$ nm (excitation at $\lambda_{exc} = 453$ nm), which originates from the conjugated structure. The emission maximum of dodecyl-PFV is significantly red-shifted as compared to unsubstituted PFV ($\lambda_{em} = 545$ nm) and hexyl-PFV ($\lambda_{em} = 560$ nm), further confirming the enhanced purity and effective conjugation of the alkyl substituted polymers (Fig. 6).

3.4. Electronic properties

Thin film cyclic voltammetry (CV) was employed to investigate the electrochemical behavior of the obtained conjugated polymers and to estimate the position of their lowest occupied molecular orbital, *viz.* the LUMO energy level or conduction band edge. The latter is possible, since the cyclic voltammograms the polymers display distinct reduction processes, *i.e.* n-doping. In marked contrast, the current density associated with the p-doping, *viz.* the oxidation processes, is very small. This n-type behavior is associated with the non-alternant polycyclic aromatic hydrocarbon units in the backbone. The conduction band edge energy level can be estimated from the onset of reduction, which for PFV, hexyl-PFV and dodecyl-PFV is located at *circa* −1.9 V *vs.* Ag/AgNO$_3$, which corresponds to a LUMO energy level at *circa* −3.1 eV. Although the HOMO energy levels are more difficult to estimate, based on the optical band gap the HOMO of the PFV-type polymers can be anticipated around −5.3 eV. From the electrochemical measurements it is clear that the introduction of an alkyl side chain has only minimal impact on the energy levels of the obtained conjugated polymers. Especially for the construction of organic solar cells, the position of the HOMO and LUMO energy levels is of interest. Currently PCBM (LUMO −3.96 eV) is the n-type material of choice for organic photovoltaic applications in combination with p-type conjugated polymers, such as P3HT. The position of the LUMO energy level in dodecyl-PPV at *circa* −3.1 eV is not as low as PCBM and it is currently still uncertain whether this polymers can replace PCBM as the electron accepting material in solar cell applications with P3HT as the p-type material. Alternatively, our dodecyl-PFV may require further tuning of the band gap energy levels or may prompt the use of an alternative p-type conjugated polymer.

Fig. 5. Temperature-dependent FT-IR spectra of the conversion of precursor polymer **7c** to dodecyl-PFV.

3.5. Mobility measurements

For an optimal performance of conjugated polymers in devices, sufficient charge carrier mobility is essential. Whereas the limited solubility and poor film forming properties of the precursor polymer of unsubstituted PFV hampers the application of this material in thin film electronic applications, our novel alkyl substituted materials can be successfully incorporated. Hence, to verify the n-type character of the materials, the charge carrier mobility in the representative with the highest purity, dodecyl-PFV, was measured in a straightforward manner using Charge Carrier Extraction by Linearly Increasing Voltage (CELIV). These measurements will provide a first estimate of the electron mobility as well as insight into the suitability of the PFV family of polymers for further device studies. CELIV is a rather novel technique used to measure the carrier mobility in semiconductors with a broad range of conductivities [40]. The advantage of this technique is that the carrier mobility can be directly measured from the experimentally recorded current transients and no data fitting procedures are required. An additional advantage of CELIV is the possibility to estimate the mobility even when rather dispersive charge carrier transport prevails. Given the experimental conditions, the charge carrier mobility can be directly estimated from the extraction maximum of the current transient [41]. Even though the carrier mobility and conductivity of the semiconducting materials can be measured in the dark, in the case of pure undoped organic semiconducting films in which the sample conductivity is low, the charge carriers can also be generated using a laser pulse. The essence of this technique is that a triangular-shaped voltage pulse is applied to the sample. The initial current step (displacement current) is caused by the geometrical capacity of the film between the two electrodes. The following increasing extraction current is caused by the photoconductivity of the sample due to the generated charge carriers. As the triangular voltage pulse continues to increase, the electric field redistribution takes place inside the sample and carrier mobility values μ can be calculated directly from the current transients.

In Fig. 7 the experimental CELIV current transients in dodecyl-PFV are shown. The capacitive current response (solid lower transient) shows rather low conductivity of the film under the given experimental conditions, which is typical for high quality undoped materials, in which the equilibrium charge carrier concentration is low. In order to photo-generate additional charge carriers, a laser pulse was
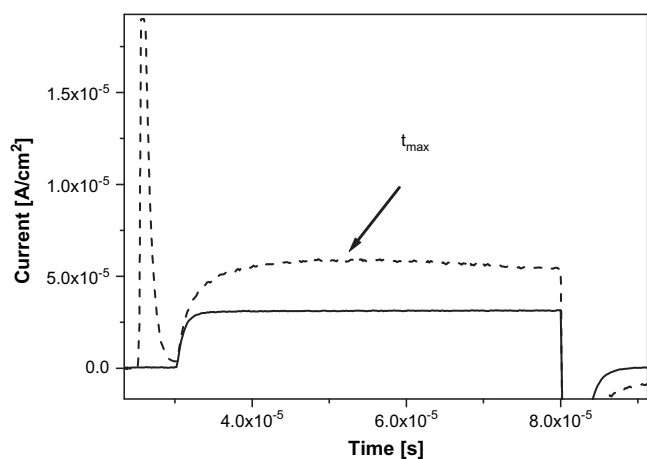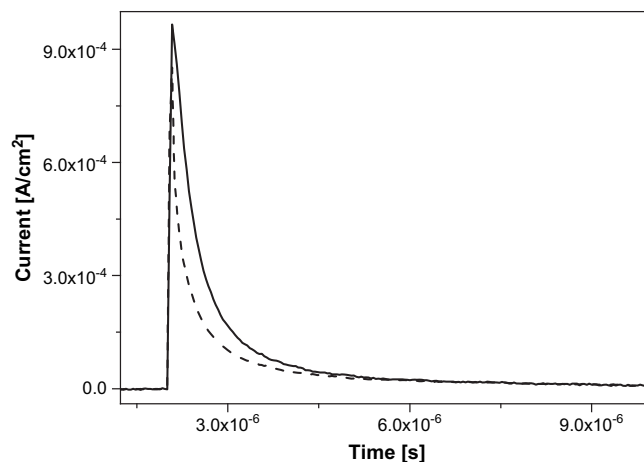
Fig. 8. Time-of-Flight photocurrent transients for electrons (solid line) and for holes (dashed line) upon illumination of the ITO contact.

applied. The extraction current transient (upper dashed transient in Fig. 7) shows rather dispersive extraction with an unpronounced extraction maximum, from which the electron mobility can directly be derived $\mu_e = 1.4 \times 10^{-4}$ cm^2/Vs. To prevent the extraction of photo-generated charge carriers prior to the application of the triangular voltage pulse, an offset voltage $U_{offset} = -0.6$ V was used. The electron mobility is measured at an electric field approximately equal to 30 kV/cm. In this context it is noteworthy that the electron mobility reported in literature for PCBM ranges from $\mu_e = 2 \times 10^{-3}$ cm^2/Vs to 4.5×10^{-3} cm^2/Vs, dependent on the measurement procedures utilized [42,43]. This demonstrates the surprisingly high electron mobility for unoptimized thin films of dodecyl-PFV, which are currently only one order of magnitude smaller than those of the most commonly applied material PCBM.

To validate the above observation and in order to determine which charge carriers, electrons or holes, are faster, an additional Hecht dependence resembling experiment was performed. To this end, the ITO electrode was illuminated under positive and negative bias. To measure the electron conduction through the film (solid transient in Fig. 8), negative bias was applied to the ITO electrode, whereas to measure the hole conduction (dashed transient in Fig. 8), positive bias was applied. As can be seen from Fig. 8, the extraction transient as well as the total extracted charge for the electrons is larger than those for the holes. Since the same amount of electrons and holes are photo-generated for both biases, the larger current would correspond to the larger carrier mobility. Therefore, it can be concluded that the electron mobility is indeed faster than the hole mobility. The high electron mobility confirms that this novel class of polymers holds significant promise for the application in plastic electronics. In this context it is noteworthy that preliminary experiments indicate that organic solar cells can be obtained using dodecyl-PPV as the n-type material as a replacement for PCBM, although further optimizations are needed.

4. Conclusion

A novel class of PPV-type polymers with a backbone structure containing fluoranthene repeating units has been developed. The presented synthetic methodology, which allows for the introduction of a variety of substituents, can be regarded as a universal synthesis route towards this class of conjugated polymers. This is exemplified by the synthesis of two substituted PFV derivatives, *i.e.* hexyl-PFV and dodecyl-PFV. It is demonstrated that PFV and its derivatives exhibit n-type behavior, which is likely associated with the non-

Fig. 7. Charge carrier extraction by linearly increasing voltage (CELIV) current transients in dodecyl-PFV: bottom transient (solid line) is the capacitive response to the applied triangle-shaped voltage pulse in the dark and the top transient (dashed line) demonstrates extraction of photogenerated charge carriers.

alternant character of the repeating units. The introduction of alkyl side chains, leads to conjugated polymers with a significantly enhanced purity as compared to unsubstituted PFV. This is a result of the fact that all synthetic intermediates, including the precursor polymers, display an improved solubility. As a result, a polymer such as dodecyl-PFV is excellently suitable for device applications. It is demonstrated using CELIV mobility measurements that dodecyl-PFV indeed has sufficiently high electron mobility for use in optical and electronic applications as an n-type material.

Acknowledgements

References

[1] Tonzola CJ, Alam MM, Kaminsky W, Jenekhe SA. J Am Chem Soc 2003;125: 13548.
[2] Ando S, Nishida J, Tada H, Inoue Y, Tokito S, Yamashita Y. J Am Chem Soc 2005; 127:5336.
[3] Ie Y, Umemoto Y, Okabe M, Kusunoki T, Nakayama K, Pu Y, et al. Org Lett 2008; 10:833.
[4] Geramita K, McBee J, Don Tilley T. J Org Chem 2009;74:820.
[5] Yu G, Heeger AJ. J Appl Phys 1995;78:4510.
[6] Granström M, Petritsch K, Arias AC, Lux A, Andersson MR, Friend RH. Nature 1998;395:257.
[7] Greenwald Y, Xu X, Fourmigué M, Srdanov G, Koss C, Wudl F, et al. J Polym Sci Part A Polym Chem 1998;36:3115.
[8] Quist PAC, Savenije TJ, Koetse MM, Veenstra SC, Kroon JM, Siebbeles LDA. Adv Funct Mater 2005;15:469.
[9] Kietzke T, Hörhold H-H, Neher D. Chem Mater 2005;17:6532.
[10] Veenstra SC, Loos J, Kroon JM. Prog Photovoltaics Res Appl 2007;15:727.
[11] Kim Y, Cook S, Choulis SA, Nelson J, Durrant JR, Bradley DDC. Chem Mater 2004;16:4812.
[12] Kim J-S, Ho PKH, Murphy CE, Friend RH. Macromolecules 2004;37:2861.
[13] McNeill CR, Watts B, Thomsen L, Belcher WJ, Greenham NC, Dastoor PC. Nano Lett 2006;6:1202.
[14] Babel A, Jenekhe SA. J Am Chem Soc 2003;125:13656.
[15] Zhu Y, Yen C-T, Jenekhe SA, Chen W-C. Macromol Rapid Commun 2004;25:1829.
[16] McNeill CR, Abrusci A, Zaumseil J, Wilson R, McKiernan MJ, Burroughes JH, et al. Appl Phys Lett 2007;90:193506/1.
[17] Hoppe H, Sariciftci NS. J Mater Res 2004;19:1924.
[18] Sheats JR. J Mater Res 2004;19:1974.
[19] Brabec CJ. Sol Energy Mater Sol Cells 2004;83:273.
[20] Thompson BC, Fréchet MJ. Angew Chem Int Ed 2008;47:58.
[21] Ramas AM, Rispens MT, van Duren JKJ, Hummelen JC, Janssen RAJ. J Am Chem Soc 2001;123:6714.
[22] Winder C, Sariciftci NS. J Mater Chem 2004:1077.
[23] Bundgaard E, Krebs FC. Sol Energy Mater Sol Cells 2007;91:954.
[24] Girotto C, Cheyns D, Aernouts T, Banishoeib F, Lutsen L, Cleij TJ, et al. Org Electron 2008;9:740.
[25] Mandoc MM, Veurman W, Koster LJA, de Boer B, Blom PWM. Adv Funct Mater 2007;17:2167.
[26] Scott LT, Cheng P, Hashemi MM, Bratcher MS, Meyer DT, Warren HB. J Am Chem Soc 1997;119:10963.
[27] Palmaerts A, Haren Mvan, Lutsen L, Cleij TJ, Vanderzande D. Macromolecules 2006;39:2438.
[28] Henckens A, Colladet K, Fourier S, Cleij TJ, Lutsen L, Gelan J, et al. Macromolecules 2005;38:19.
[29] Henckens A, Duyssens I, Lutsen L, Vanderzande D, Cleij TJ. Polymer 2006; 47:123.
[30] Nguyen LH, Günes S, Neugebauer H, Sariciftci NS, Banishoeib F, Henckens A, et al. Sol Energy Mater Sol Cells 2006;90:2815.
[31] Banishoeib F, Adriaensens P, Berson S, Guillerez S, Douheret O, Manca JV, et al. Sol Energy Mater Sol Cells 2007;91:1026.
[32] Banishoeib F, Henckens A, Fourier S, Vanhooyland G, Breselge M, Manca JV, et al. Thin Solid Films 2008;516:3978.
[33] Jørgensen M, Norrman K, Krebs FC. Sol Energy Mater Sol Cells 2008;92:686.
[34] Bjerring M, Nielsen JS, Nielsen NC, Krebs FC. Macromolecules 2007;40:6012.
[35] Gevorgyan SA, Krebs FC. Chem Mater 2008;20:4386.
[36] Petersen MH, Gevorgyan SA, Krebs FC. Macromolecules 2008;41:8986.
[37] Behnisch B, Martinez-Ruiz P, Schweikart K, Hanack M. Eur J Org Chem 2000:2541.
[38] Eckhardt H, Shacklette LW, Jen KY, Elsenbaumer RL. J Chem Phys 1989; 91:1303.
[39] Kesters E, Vanderzande D, Lutsen L, Penxten H, Carleer R. Macromolecules 2005;38:1141.
[40] Juska G, Arlauskas K, Viliunas M, Kocka. J. Phys Rev Lett 2000;84:4946.
[41] Österbacka R, Pivrikasa A, Juska G, Genevicius K, Arlauskas K, Stubb H. Curr Appl Phys 2004;4:534.
[42] Hummelen JC, Mihailetchi VD, Duren KJ, Blom PWM, Janssen RAJ, Kroon JM, et al. Adv Funct Mater 2003;13:43.
[43] Waldauf C, Scilinsky P, Perisutti M, Hauch J, Brabec CJ. Adv Mater 2003; 15:2084.